 CMES, vol.80, no.1, pp.57-86, 2011

# A Revision of Relaxed Steepest Descent Method from the Dynamics on an Invariant Manifold

**Chein-Shan Liu**[1]

**Abstract:** Based-on the ordinary differential equations defined on an invariant manifold, we propose a theoretical procedure to derive a Relaxed Steepest Descent Method (RSDM) for numerically solving an ill-posed system of linear equations when the data are polluted by random noise. The invariant manifold is defined in terms of a squared-residual-norm and a fictitious time-like variable, and in the final stage we can derive an iterative algorithm including a parameter, which is known as the relaxation parameter. Through a Hopf bifurcation, this parameter indeed plays a major role to switch the situation of slow convergence to a new situation with faster convergence. Several numerical examples, including the first-kind Fredholm integral equation and backward heat conduction problem, are examined and compared with exact solutions, revealing that the RSDM has superior computational efficiency and accuracy even for the highly ill-conditioned linear equations with a large noise imposed on the given data.

**Keywords:** Ill-posed linear equations, Relaxed Steepest Descent Method (RSDM), Invariant manifold, Barzilai-Borwein method

## 1 Introduction

In this paper we propose a robust and easily-implemented algorithm to solve the following linear equations system:

$$\mathbf{Bx} = \mathbf{b}, \tag{1}$$

where $\mathbf{B} \in \mathbb{R}^{n\times n}$ is a given matrix, which might be unsymmetric, and $\mathbf{x} \in \mathbb{R}^n$ is an unknown vector determined from the input data $\mathbf{b} \in \mathbb{R}^n$. When $\mathbf{B}$ is severely ill-conditioned and $\mathbf{b}$ is perturbed by noise, we will encounter the problem that the numerical solution of Eq. (1) may deviate from the exact one to a great extent. Therefore, an algorithm compromises stabilty, efficiency and accuracy is desired.

[1] Department of Civil Engineering, National Taiwan University, Taipei, Taiwan. E-mail: liucs@ntu.edu.tw

To overcome the sensitivity to noise it is usually using a regularization method to solve this sort of ill-posed problem [Kunisch and Zou (1998); Wang and Xiao (2001), Xie and Zou (2002), Resmerita (2005)], where a suitable regularization parameter is used to depress the bias in the computed solution by a better balance of approximation error and propagated data error. There are several regularization techniques developed after the pioneer work of Tikhonov and Arsenin (1977). Previously, the author and his coworkers have developed several methods to solve the ill-posed linear problems, like that using the fictitious time integration method as a filter for ill-posed linear system [Liu and Atluri (2009a)], a modified polynomial expansion method [Liu and Atluri (2009b)], the Laplacian conditioners [Liu, Yeih and Atluri (2009)], the nonstandard group preserving scheme [Liu (2005)], as well as a natural regularization method [Liu, Hong and Atluri (2010)].

It is known that iterative methods for solving the system of algebraic equations can be derived from the discretization of a certain ODEs system [Bhaya and Kaszkurewicz (2006); Chehab and Laminie (2005); Hoang and Ramm (2008, 2010); Liu and Atluri (2008)]. Particularly, some descent methods can be interpreted as the discretizations of gradient flows [Brown and Bartholomew-Biggs (1989); Helmke and Moore (1994)]. For a large scale system the main choice is using an iterative regularization algorithm, where a regularization parameter is presented by the number of iterations. The iterative method works if an early stopping criterion is used to prevent the reconstruction of noisy components in the approximate solutions.

After the work by Liu and Atluri (2008), there were several works applied the fictitious time integration method (FTIM) to solve engineering problems, e.g., Liu and Atluri (2009a), Liu (2008, 2009a, 2009b, 2009c, 2010), Chi, Yeih and Liu (2009), Ku, Yeih, Liu and Chi (2009) and Chang and Liu (2009).

## 2 An invariant manifold based-on residual-norm

There are several regularization methods to deal with Eq. (1) when $\mathbf{B}$ is ill-conditioned, of which the most prominent and best well understood are the Tikhonov method, the Landweber iteration method, and truncated singular value decomposition, all being linear and all being strongly convergent with an appropriate a priori parameter choice [Eicke, Louis and Plato (1990)]. In this paper we consider an iterative regularization method for Eq. (1) by investigating

$$\mathbf{F}(\mathbf{x}) = \mathbf{B}\mathbf{x} - \mathbf{b}. \tag{2}$$

We start from a continuous manifold [Absil, Baker and Gallivan (2007); Adler, Dedieu, Margulies, Martens and Shub (2002); Baker, Absil and Gallivan (2008);

Luenberger (1972); Smith (1994); Yang (2007)], defined in terms of the squared-residual-norm of $\mathbf{F}$ and a function $Q(t)$:

$$h(\mathbf{x},t) := \frac{1}{2}Q(t)\|\mathbf{F}(\mathbf{x})\|^2 = C. \tag{3}$$

Here, we let $\mathbf{x}$ be a function of a fictitious time-like variable $t$. We do not need to specify the function $Q(t)$ a priori, of which $\sqrt{2C/Q(t)}$ is merely a time-evolving measure of the residual error $\|\mathbf{F}(\mathbf{x})\|$. Hence, we expect that in our algorithm $Q(t) > 0$ is an increasing function of $t$, and the residual error can be decreased with time. We let $Q(0) = 1$, and $C$ is determined by the initial condition $\mathbf{x}(0) = \mathbf{x}_0$ given by

$$C = \frac{1}{2}\|\mathbf{F}(\mathbf{x}_0)\|^2. \tag{4}$$

Usually, $C > 0$, and $C = 0$ when the initial value $\mathbf{x}_0$ is just the solution of Eq. (2).

When $C > 0$ and $Q > 0$, the manifold defined by Eq. (3) is continuous and differentiable, and thus the following differential operation carried out on the manifold makes sense. For the requirement of "consistency condition", i.e., $\mathbf{x}(t)$ always on the manifold in time, we have

$$\frac{1}{2}\dot{Q}(t)\|\mathbf{F}(\mathbf{x})\|^2 + Q(t)(\mathbf{B}^{\mathrm{T}}\mathbf{F})\cdot\dot{\mathbf{x}} = 0, \tag{5}$$

which is obtained by taking the time differential of Eq. (3) with respect to $t$ and considering $\mathbf{x} = \mathbf{x}(t)$.

The governing equation of $\mathbf{x}$ cannot be uniquely determined by Eq. (5); however, we suppose that $\mathbf{x}$ is governed by a gradient-flow, like that for the steepest-descent method (SDM):

$$\dot{\mathbf{x}} = -\lambda\frac{\partial h}{\partial \mathbf{x}} = -\lambda Q(t)\mathbf{B}^{\mathrm{T}}\mathbf{F}, \tag{6}$$

where $\lambda$ is to be determined. Inserting Eq. (6) into Eq. (5) we can solve

$$\lambda = \frac{\dot{Q}(t)\|\mathbf{F}\|^2}{2Q^2(t)\|\mathbf{B}^{\mathrm{T}}\mathbf{F}\|^2}. \tag{7}$$

Thus by inserting the above $\lambda$ into Eq. (6) we can obtain an ODEs system for $\mathbf{x}$:

$$\dot{\mathbf{x}} = -q(t)\frac{\|\mathbf{F}\|^2}{\|\mathbf{B}^{\mathrm{T}}\mathbf{F}\|^2}\mathbf{B}^{\mathrm{T}}\mathbf{F}, \tag{8}$$

where

$$q(t) := \frac{\dot{Q}(t)}{2Q(t)}. \tag{9}$$

If $Q(t)$ can be guaranteed to be an increasing function of $t$, we have an absolutely convergent numerical method in solving Eq. (1):

$$\|\mathbf{F}(\mathbf{x})\|^2 = \frac{2C}{Q(t)}. \tag{10}$$

When $t$ is large enough the above equation will enforce the residual error $\|\mathbf{F}(\mathbf{x})\|$ to tend to zero, and meanwhile the solution of Eq. (1) is obtained approximately.

## 3 The dynamics on invariant manifold

Equation (8) is an ODEs system defined on the invariant manifold (10). However, how to realize it needs the following further studies.

### *3.1 Keeping* x *on the manifold*

In order to keep $\mathbf{x}$ on the manifold defined by Eq. (10) we can consider the evolution of $\mathbf{F}$ along the path $\mathbf{x}(t)$ by

$$\dot{\mathbf{F}} = \mathbf{B}\dot{\mathbf{x}} = -q(t)\frac{\|\mathbf{F}\|^2}{\|\mathbf{B}^{\mathrm{T}}\mathbf{F}\|^2}\mathbf{A}\mathbf{F}, \tag{11}$$

where

$$\mathbf{A} := \mathbf{B}\mathbf{B}^{\mathrm{T}}. \tag{12}$$

We simply use the Euler scheme to integrate Eq. (11):

$$\mathbf{F}(t+\Delta t) = \mathbf{F}(t) - \Delta t q(t)\frac{\|\mathbf{F}\|^2}{\|\mathbf{B}^{\mathrm{T}}\mathbf{F}\|^2}\mathbf{A}\mathbf{F}. \tag{13}$$

Taking the square-norms of both the sides and using Eq. (10) we can obtain

$$\frac{2C}{Q(t+\Delta t)} = \frac{2C}{Q(t)} - 2\Delta t\frac{2Cq(t)}{Q(t)}\frac{\mathbf{F}\cdot(\mathbf{A}\mathbf{F})}{\|\mathbf{B}^{\mathrm{T}}\mathbf{F}\|^2} + (\Delta t)^2\frac{2Cq^2(t)}{Q(t)}\frac{\|\mathbf{F}\|^2}{\|\mathbf{B}^{\mathrm{T}}\mathbf{F}\|^4}\|\mathbf{A}\mathbf{F}\|^2, \tag{14}$$

and thus the following scalar equation:

$$a(\Delta t)^2 - b\Delta t + 1 - \frac{Q(t)}{Q(t+\Delta t)} = 0, \tag{15}$$

where

$$a := q^2(t)\frac{\|\mathbf{F}\|^2\|\mathbf{AF}\|^2}{\|\mathbf{B}^{\mathrm{T}}\mathbf{F}\|^4}, \tag{16}$$

$$b := 2q(t). \tag{17}$$

### *3.2 A novel method*

Inserting Eqs. (16) and (17) into Eq. (15) we can derive

$$a_0(q\Delta t)^2 - 2(q\Delta t) + 1 - s = 0, \tag{18}$$

where

$$s = \frac{Q(t)}{Q(t+\Delta t)}, \tag{19}$$

$$a_0 := \frac{\|\mathbf{F}\|^2\|\mathbf{AF}\|^2}{\|\mathbf{B}^{\mathrm{T}}\mathbf{F}\|^4} \geq 1, \tag{20}$$

by using the Cauchy-Schwarz inequality:

$$\|\mathbf{B}^{\mathrm{T}}\mathbf{F}\|^2 = \mathbf{F}\cdot(\mathbf{AF}) \leq \|\mathbf{F}\|\|\mathbf{AF}\|.$$

From Eq. (18), we can take the solution of $q\Delta t$ to be

$$q\Delta t = \frac{1-\sqrt{1-(1-s)a_0}}{a_0}, \text{ if } 1-(1-s)a_0 \geq 0. \tag{21}$$

Let

$$1-(1-s)a_0 = \gamma^2 \geq 0, \;\; s = 1 - \frac{1-\gamma^2}{a_0}. \tag{22}$$

Thus we have

$$q\Delta t = \frac{1-\gamma}{a_0}. \tag{23}$$

Similarly, by applying the Euler method to Eq. (8) and using the above equation we can obtain the following algorithm:

$$\mathbf{x}(t+\Delta t) = \mathbf{x}(t) - \eta\frac{\|\mathbf{B}^{\mathrm{T}}\mathbf{F}\|^2}{\|\mathbf{AF}\|^2}\mathbf{B}^{\mathrm{T}}\mathbf{F}, \tag{24}$$

where

$$\eta = 1 - \gamma \tag{25}$$

is a parameter with $0 \leq \gamma < 1$ and $0 < \eta \leq 1$. Under the above condition and Eqs. (19), (20) and (22) we can prove that the new algorithm satisfies

$$\frac{\|\mathbf{F}(t+\Delta t)\|}{\|\mathbf{F}(t)\|} = \sqrt{s} < 1, \tag{26}$$

which means that the residual error is absolutely decreased, and thus it is a monotone decreasing algorithm [Liu and Atluri (2011)].

### *3.3 A relaxed steepest descent method*

Without resorting on the time-like variable $t$, we can let $\mathbf{x}_k$ denote the numerical value of $\mathbf{x}$ at the $k$-th step. Thus, we arrive at a purely iterative algorithm:

$$\mathbf{x}_{k+1} = \mathbf{x}_k - (1-\gamma)\frac{\|\mathbf{B}^{\mathrm{T}}\mathbf{F}_k\|^2}{\|\mathbf{A}\mathbf{F}_k\|^2}\mathbf{B}^{\mathrm{T}}\mathbf{F}_k, \tag{27}$$

where the convergence rate is given by

$$\frac{1}{s_k} = \frac{a_k}{a_k - 1 + \gamma^2} > 1, \tag{28}$$

$$a_k = \frac{\|\mathbf{F}_k\|^2\|\mathbf{A}\mathbf{F}_k\|^2}{\|\mathbf{B}^{\mathrm{T}}\mathbf{F}_k\|^4}. \tag{29}$$

Then, we can derive the following algorithm:

(i) Give an initial $\mathbf{x}_0$, and then $\mathbf{F}_0 = \mathbf{B}\mathbf{x}_0 - \mathbf{b}$.

(ii) For $k = 0, 1, 2\ldots$, we repeat the following computations:

$$\mathbf{x}_{k+1} = \mathbf{x}_k - (1-\gamma)\frac{\|\mathbf{B}^{\mathrm{T}}\mathbf{F}_k\|^2}{\|\mathbf{A}\mathbf{F}_k\|^2}\mathbf{B}^{\mathrm{T}}\mathbf{F}_k, \tag{30}$$

$$\mathbf{F}_{k+1} = \mathbf{B}\mathbf{x}_{k+1} - \mathbf{b}. \tag{31}$$

If $\|\mathbf{F}_{k+1}\| < \varepsilon$ then stop; otherwise, go to step (ii). Here, $0 \leq \gamma < 1$ is a parameter determined by the user.

Solving Eq. (1) by the steepest descent method is equivalent to solving the following minimization problem:

$$\min_{\mathbf{x}\in\mathbb{R}^n} \varphi(\mathbf{x}) = \min_{\mathbf{x}\in\mathbb{R}^n} \left[ \frac{1}{2}\mathbf{x}^{\mathrm{T}}\mathbf{C}\mathbf{x} - \mathbf{b}_1^{\mathrm{T}}\mathbf{x} \right], \tag{32}$$

where

$$\mathbf{C} := \mathbf{B}^{\mathrm{T}}\mathbf{B}, \;\; \mathbf{b}_1 := \mathbf{B}^{\mathrm{T}}\mathbf{b}. \tag{33}$$

Thus one can derive the following steepest descent method (SDM):
(i) Give an initial $\mathbf{x}_0$.
(ii) For $k = 0, 1, 2, \ldots$, we repeat the following computations:

$$\mathbf{r}_k = \mathbf{C}\mathbf{x}_k - \mathbf{b}_1, \tag{34}$$

$$\mathbf{x}_{k+1} = \mathbf{x}_k - \frac{\|\mathbf{r}_k\|^2}{\mathbf{r}_k^{\mathrm{T}}\mathbf{C}\mathbf{r}_k}\mathbf{r}_k. \tag{35}$$

If $\mathbf{x}_{k+1}$ converges according to a given stopping criterion $\|\mathbf{r}_{k+1}\| < \varepsilon$, then stop; otherwise, go to step (ii).

Because of $\mathbf{r}_k = \mathbf{B}^{\mathrm{T}}\mathbf{F}_k$ and $\mathbf{A} = \mathbf{B}\mathbf{B}^{\mathrm{T}}$, the algorithm (30) is equivalent to the algorithm (35), in addition to a relaxation parameter $1-\gamma$ appeared in Eq. (30). Thus, we can call the algorithm (30) a *relaxed steepest descent method* (RSDM) endowed with a *relaxation parameter* $\gamma$ determined by the user [Hanke (1991, 1995)]. Up to here a *theoretical foundation of the relaxed steepest descent method is given from the dynamics evolving on an invariant manifold.*

### *3.4 If* **B** *is a positive matrix*

If **B** is a positive matrix, we can solve

$$\mathbf{F} = \mathbf{B}^{1/2}\mathbf{x} - \mathbf{B}^{-1/2}\mathbf{b} = \mathbf{0}. \tag{36}$$

Correspondingly, we can derive the following iterative algorithm:

$$\mathbf{x}_{k+1} = \mathbf{x}_k - \eta \frac{\|\mathbf{r}_k\|^2}{\mathbf{r}_k^{\mathrm{T}}\mathbf{B}\mathbf{r}_k}\mathbf{r}_k, \tag{37}$$

where

$$\mathbf{r}_k = \mathbf{B}\mathbf{x}_k - \mathbf{b}, \tag{38}$$

$$\eta = \gamma_1 \exp\left[ -\frac{\gamma_2\|\mathbf{r}_k\|}{\|\mathbf{x}_k\|} \right], \tag{39}$$

$$a_k = \frac{\|\mathbf{F}_k\|^2\mathbf{r}_k^{\mathrm{T}}\mathbf{B}\mathbf{r}_k}{\|\mathbf{r}_k\|^4}. \tag{40}$$

Barzilai and Borwein (1988) were able to produce a substantial improvement of the convergence speed for the linear problem in Eq. (1) with **B** being positive by using the Barzilai-Borwein method (BBM):

$$\mathbf{x}_{k+1} = \mathbf{x}_k - \frac{(\Delta\mathbf{r}_{k-1})^{\mathrm{T}}\Delta\mathbf{x}_{k-1}}{\|\Delta\mathbf{r}_{k-1}\|^2}\mathbf{r}_k, \tag{41}$$

where $\Delta\mathbf{r}_{k-1} = \mathbf{r}_k - \mathbf{r}_{k-1}$, and $\Delta\mathbf{x}_{k-1} = \mathbf{x}_k - \mathbf{x}_{k-1}$. Initially, we can set $\mathbf{r}_0 = \mathbf{0}$ and $\mathbf{x}_0 = \mathbf{0}$.

## 4 Numerical examples

In order to assess the performance of the newly developed method of the RSDM, let us investigate the following examples. Some results are compared with those obtained by the singular value decomposition (SVD), non-standard group preserving scheme (NGPS), fictitious time integration method (FTIM) [Liu and Atluri (2008)], steepest descent method (SDM), conjugate gradient method (CGM), the Barzilai-Borwein method (BBM), and the Tikhonov regularization (TR). While the NGPS and FTIM are reported by Liu and Chang (2009), the TR is reported by Liu, Hong and Atluri (2010).

### *4.1 Hilbert problems*

Finding an $n$-degree polynomial function $p(x) = a_0 + a_1 x + \ldots + a_n x^n$ to best match a continuous function $f(x)$ in the interval of $x \in [0,1]$:

$$\min_{\deg(p)\le n} \int_0^1 [f(x) - p(x)]^2 dx, \tag{42}$$

leads to a problem governed by Eq. (1), where **B** is the $(n+1)\times(n+1)$ Hilbert matrix, defined by

$$B_{ij} = \frac{1}{i+j-1}, \tag{43}$$

**x** is composed of the $n+1$ coefficients $a_0, a_1, \ldots, a_n$ appeared in $p(x)$, and

$$\mathbf{b} = \begin{bmatrix} \int_0^1 f(x)dx \\ \int_0^1 xf(x)dx \\ \vdots \\ \int_0^1 x^n f(x)dx \end{bmatrix} \tag{44}$$

is uniquely determined by the function $f(x)$.

The Hilbert matrix is a famous example of highly ill-conditioned matrices. Eq. (1) with the coefficient matrix **B** having a large condition number usually displays that an arbitrarily small perturbation of data on the right-hand side may lead to an arbitrarily large perturbation to the solution on the left-hand side.

In this example we consider a highly ill-conditioned linear equation (1) with **B** given by Eq. (43). The ill-posedness of Eq. (1) with the above **B** increases very fast with an exponential growth with $n$.

#### *4.1.1 $n = 9$ (Example 1)*

In order to compare the numerical solutions with exact solutions we suppose that $x_1 = x_2 = \ldots = x_n = 1$ to be the exact one, and then by Eq. (43) we have

$$b_i = \sum_{j=1}^{n} \frac{1}{i+j-1} + \sigma R(i), \tag{45}$$

where we consider noise being imposed on the data with random numbers $R(i) \in [-1,1]$.

We first calculate this problem for the case with $n = 9$ and $\sigma = 0$. The resulting linear equation is highly ill-conditioned, since the condition number is quite large, up to $4.93 \times 10^{11}$.

In the computation by the RSDM we have fixed $\gamma = 0.06$. Starting from $x_1 = \ldots = x_9 = 0.5$, we employ the iterative algorithm in Section 3.3 to this problem with a stopping criterion $\varepsilon = 10^{-8}$. Through 50000 iterations the numerical solution converges to the exact solution very accurately as shown in Table 1 with the maximum error $1.44 \times 10^{-3}$, where, for the purpose of comparison, the values obtained by the singular value decomposition (SVD) technique [Press, Teukolsky, Vetterling and Flannery (1992)] are also listed.

When we apply the CGM to this problem we find that it is very sensitive to the noise; indeed, under a moderate noise level $\sigma = 10^{-5}$ we cannot compute the solution by using the CGM. In the computation of this noisy problem by the RSDM, the numerical solution converges to the exact solution very accurately as shown in Table 2 with the maximum error $1.29 \times 10^{-2}$. We also apply the Barzilai-Borwein method (BBM) to this problem under the same noise. When the convergence criterion is set smaller than $\varepsilon = 10^{-4}$, the BBM is unstable and gave incorrect results. Under the above convergence criterion the BBM converges very fast with 17 steps, and the maximum error is $3.08 \times 10^{-2}$. It can be seen that the accuracy of RSDM is better than SDM and BBM.

Table 1: Comparing the numerical results for Example 1 with different methods

| Solutions | $x_1$ | $x_2$ | $x_3$ | $x_4$ | $x_5$ | $x_6$ | $x_7$ | $x_8$ | $x_9$ |
|---|---|---|---|---|---|---|---|---|---|
| Exact | 1.0 | 1.0 | 1.0 | 1.0 | 1.0 | 1.0 | 1.0 | 1.0 | 1.0 |
| SVD | 0.9999 | 1.008 | 0.985 | 0.995 | 1.007 | 1.012 | 1.009 | 0.999 | 0.984 |
| NGPS | 1.00001 | 0.99980 | 1.00090 | 0.99909 | 0.99928 | 1.00037 | 1.00105 | 1.00062 | 0.99887 |
| FTIM | 1.00001 | 0.99981 | 1.00082 | 0.99922 | 0.99933 | 1.00029 | 1.00092 | 1.00058 | 0.99901 |
| SDM | 1.00001 | 0.99980 | 1.00091 | 0.99910 | 0.99928 | 1.00035 | 1.00103 | 1.00062 | 0.99898 |
| CGM | 1.00000 | 1.00001 | 0.99924 | 1.00019 | 0.99988 | 0.99985 | 1.00008 | 1.00019 | 0.99987 |
| RSDM | 1.00000 | 0.99986 | 1.00087 | 0.99888 | 0.99928 | 1.00058 | 1.00128 | 1.00066 | 0.99856 |

Table 2: Comparing the numerical results for Example 1 under a noise with zero-mean

| Solutions | $x_1$ | $x_2$ | $x_3$ | $x_4$ | $x_5$ | $x_6$ | $x_7$ | $x_8$ | $x_9$ |
|---|---|---|---|---|---|---|---|---|---|
| Exact | 1.0 | 1.0 | 1.0 | 1.0 | 1.0 | 1.0 | 1.0 | 1.0 | 1.0 |
| NGPS | 1.00016 | 1.00038 | 0.99902 | 0.99119 | 1.00490 | 1.01430 | 1.00135 | 0.99808 | 0.98977 |
| FTIM | 1.00021 | 1.00074 | 0.99568 | 0.99464 | 1.00761 | 1.00961 | 1.00572 | 0.99771 | 0.98689 |
| SDM | 1.00102 | 0.97669 | 1.12472 | 0.79421 | 1.00401 | 1.19965 | 0.93218 | 0.98919 | 0.97715 |
| BBM | 1.00453 | 0.97562 | 1.00597 | 1.01831 | 1.02055 | 1.01301 | 1.00051 | 0.98544 | 0.96922 |
| RSDM | 0.99961 | 1.00573 | 0.98751 | 0.99722 | 1.00698 | 1.01005 | 1.00663 | 0.99843 | 0.98708 |

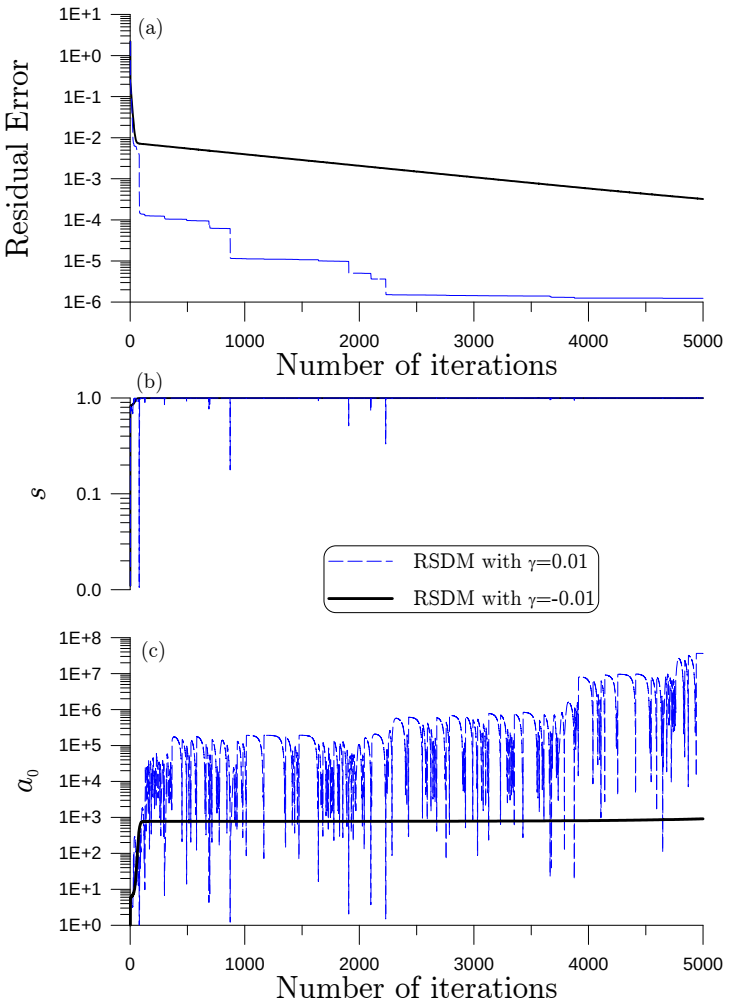


Figure 1: For example 1 comparing (a) the residual errors, (b) $s$, and (c) $a_0$ by the RSDM with different $\gamma$.

Now, we explain the parameter $\gamma$ appeared in Eq. (30). In Fig. 1 we compare residual errors, $s$ and $a_0$ for $\gamma = -0.01$ and $\gamma = 0.01$. From Fig. 1(c) it can be seen that for the case with $\gamma = -0.01$, the values of $a_0$ tend to a constant and keep unchanged. By Eq. (20) it means that there exists an attracting set for the iterative orbit of $\mathbf{x}$ described by the following manifold:

$$\frac{\|\mathbf{F}\|^2\|\mathbf{AF}\|^2}{\|\mathbf{B}^{\mathrm{T}}\mathbf{F}\|^4} = \text{Constant}. \tag{46}$$

Upon the iterative orbit approaches to this *slow manifold*, the residual error is slowly reduced as shown in Fig. 1(a) by the solid line, wherea the ratio of $s$ is also keeping near to 1 as shown in Fig. 1(b) by the solid line. Conversely, for the case $\gamma = 0.01$, $a_0$ is no more tending to a constant as shown in Fig. 1(c) by the dashed line. Because the iterative orbit is not attracted by a slow manifold, the residual error as shown in Fig. 1(a) by the dashed line can be reduced step by step, wherea the ratio of $s$ is sometimes leaving the value that near to 1 as shown in Fig. 1(b) by the dashed line. For the latter case the new algorithm can give very accurate numerical solution with a residual error tending to $10^{-6}$. Thus we can observe that when $\gamma$ varies from a negative value to a positive value, the iterative dynamics given by Eq. (30) undergoes a Hopf bifurcation, like as the ODEs behavior observed by Liu (2001, 2007). The original stable manifold existent for $\gamma = -0.01$ now becomes a ghost manifold for $\gamma = 0.01$, and thus the orbit generated from the case $\gamma = 0.01$ is not attracted by that manifold again, and instead of the intermittency occupies, leading to an irregularly jumping behavior of $a_0$ as shown in Fig. 1(c) by the dashed line.

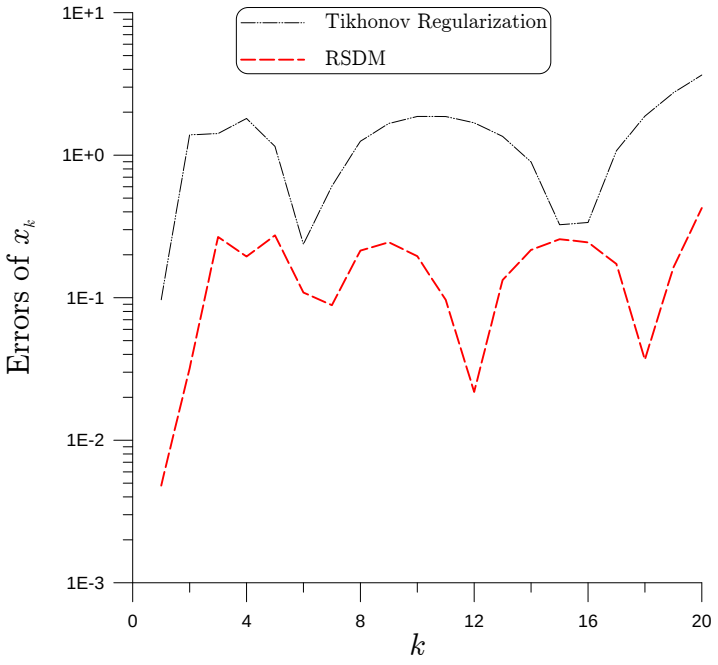


Figure 2: For a Hilbert linear system with $n = 20$ comparing the numerical errors of the Tikhonov regularization, and the RSDM.

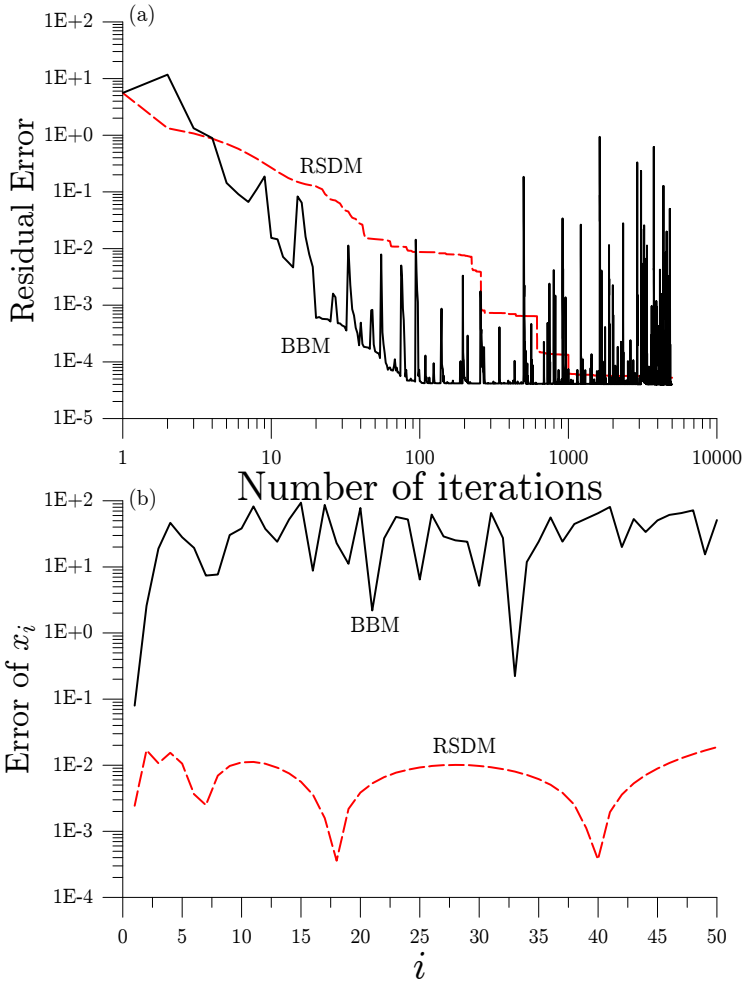


Figure 3: For example 3 of a Hilbert linear system with constant solution: (a) comparing the residual errors of RSDM and BBM, and (b) showing the numerical errors.

### *4.1.2 $n = 20$ (Example 2)*

Starting from an initial value of $\mathbf{x}_0 = \mathbf{1}$, we apply the RSDM with $\gamma = 0.08$ to solve the linear system (1) with the Hilbert matrix as a coefficient matrix, where a random noise with intensity $\sigma = 0.001$ and mean 0.5 is added in the data on the right-hand side of $\mathbf{b}$. We let $x_i = i,\ i = 1,\ldots,20$ be the exact solutions, and the numerical results are compared in Fig. 2 with the Tikhonov regularization with $\alpha = 10^{-5}$. One can see that the RSDM is more accurater than the Tikhonov regularization (TR).

#### 4.1.3 $n = 50$ (Example 3)

Let us increase the ill-posedness of this problem with $n = 50$. For this problem the condition number is about $1.1748 \times 10^{19}$. We first consider a constant solution $x_1 = x_2 = \ldots = x_{50} = 1$. The noise $\sigma$ and the convergence criterion $\varepsilon$ are both fixed to be $10^{-5}$. Starting from the initial condition $x_i = 0.5,\ i = 1, \ldots, 50$, both the RSDM and BBM over 5000 iterations do not converge as shown in Fig. 3(a) for the residual errors and Fig. 3(b) for the numerical errors. The RSDM can get an approximate solution, but the BBM leads to an incorrect solution.

Then, we consider a more complex solution:

$$\begin{aligned} x_i &= 2\sin(p_i)\exp[p_i(1-p_i)], \quad p_i = i \times \frac{1}{n}, \\ b_i &= \sum_{j=1}^{n} \frac{1}{i+j-1} x_j + \sigma R(i), \end{aligned} \tag{47}$$

with $n = 50$ and $0 < p_i \leq 1$. This noise has a mean value 0.5. This problem is more difficult than the above two problems with constant $x_1 = \ldots = x_n$.

When the noise is imposed in the levels of $\sigma = 10^{-4}$ and $\sigma = 10^{-2}$, the RSDM is still applicable. In Fig. 4(a) we compare the exact solution given in Eq. (47) with the numerical solution obtained from the RSDM by using $\gamma = 0.05$, which runs 2000 steps. In Fig. 4(b) we compare the exact solution with the numerical solution under $\gamma = 0.07$ and $\sigma = 10^{-2}$. At the two ends there are large discrepancies with the maximum error about 0.283. With a noise larger than $\sigma = 10^{-8}$, both the SDM and CGM are not applicable.

### 4.2 Example 4

When the backward heat conduction problem (BHCP) is considered in a spatial interval of $0 < x < \ell$ by subjecting to the boundary conditions at two ends of a slab:

$$u_t(x,t) = \alpha u_{xx}(x,t), \quad 0 < t < T, \quad 0 < x < \ell, \tag{48}$$

$$u(0,t) = u_0(t), \quad u(\ell,t) = u_\ell(t), \tag{49}$$

we solve $u$ under a final time condition:

$$u(x,T) = u^T(x). \tag{50}$$

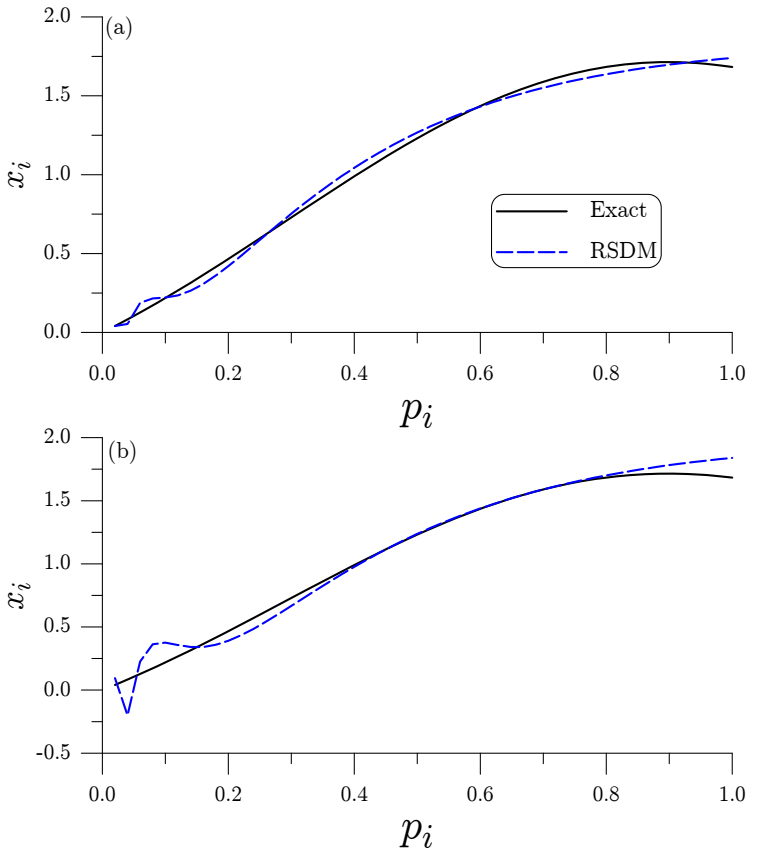


Figure 4: Comparing the numerical solutions of RSDM with a non-constant exact solution for example 3 with $n = 50$: (a) $\sigma = 0.0001$, and (b) $\sigma = 0.01$.

The fundamental solution to Eq. (48) is given as follows:

$$K(x,t) = \frac{H(t)}{2\sqrt{\alpha\pi t}} \exp\left(\frac{-x^2}{4\alpha t}\right), \tag{51}$$

where $H(t)$ is the Heaviside function.

The method of fundamental solutions (MFS) has a broad application in engineering computations. However, the MFS has a serious drawback in that the resulting system of linear equations is always highly ill-conditioned, when the number of source points is increased [Golberg and Chen (1996)], or when the distances of source points are increased [Chen, Cho and Golberg (2006)].

In the MFS the solution of $u$ at the field point $z = (x,t)$ can be expressed as a linear

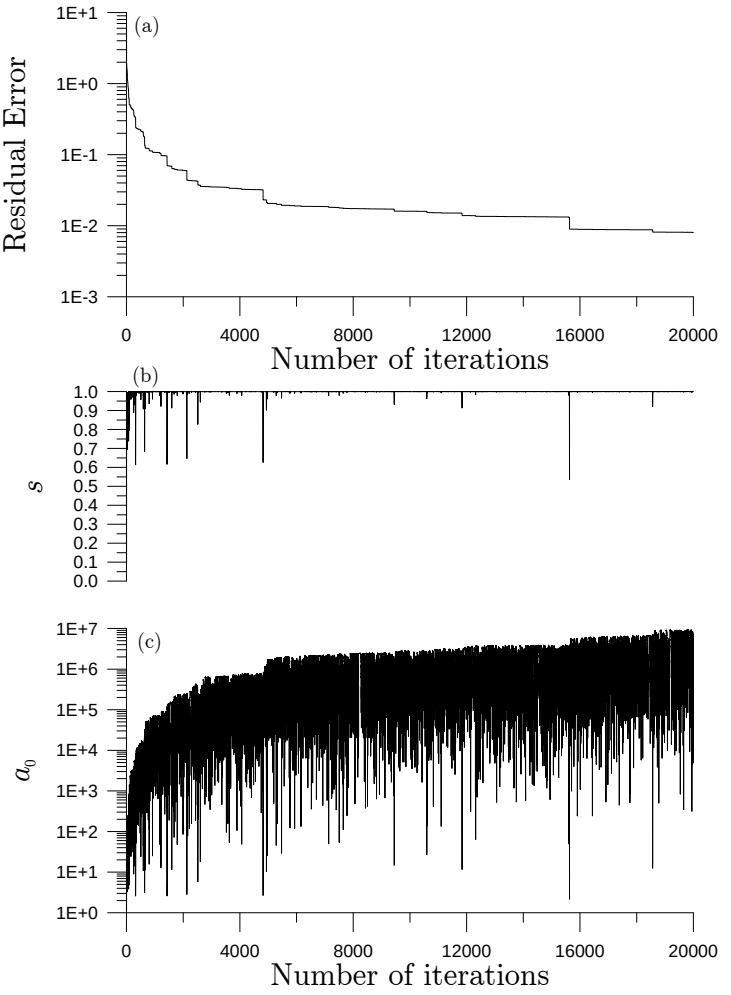


Figure 5: For example 4 showing (a) the residual errors, (b) $s$, and (c) $a_0$ for constant $\eta$.

combination of the fundamental solutions $U(z,s_j)$:

$$u(z)=\sum_{j=1}^{N} c_j U(z,s_j),\ \ s_j=(\eta_j,\tau_j)\in\Omega^c, \tag{52}$$

where $N$ is the number of source points, $c_j$ are unknown coefficients, and $s_j$ are source points located in the complement $\Omega^c$ of $\Omega=[0,\ell]\times[0,T]$. For the heat

conduction equation we have the basis functions

$$U(z,s_j) = K(x-\eta_j, t-\tau_j). \tag{53}$$

It is known that the location of source points in the MFS has a great influence on the accuracy and stability. In a practical application of MFS to solve the BHCP, the source points are uniformly located on two straight lines, which was adopted by Hon and Li (2009) and Liu (2011), showing a large improvement than the line location of source points below the initial time. After imposing the boundary conditions and the final time condition on Eq. (52) we can obtain a linear equations system:

$$\mathbf{Bx} = \mathbf{b}, \tag{54}$$

where

$$\begin{aligned} &B_{ij} = U(z_i,s_j),\ \ \mathbf{x} = (c_1,\cdots,c_N)^{\mathrm{T}}, \\ &\mathbf{b} = (u_\ell(t_i),\ i=1,\ldots,m_1; u^T(x_j),\ j=1,\ldots,m_2; u_0(t_k),\ k=m_1,\ldots,1)^{\mathrm{T}}. \end{aligned} \tag{55}$$

The number $n = 2m_1 + m_2$ of collocation points does not necessarily equal to the number $N$ of source points.

Since the BHCP is highly ill-posed, the ill-conditioning of the matrix $\mathbf{B}$ in Eq. (54) is serious. To overcome the ill-posedness of Eq. (54) we can employ the RSDM to solve this problem. Here we compare the numerical solution with an exact solution:

$$u(x,t) = \cos(\pi x)\exp(-\pi^2 t).$$

For the case with $T = 1$ the value of final data is in the order of $10^{-4}$, which is small in a comparison with the value of the initial temperature $u_0(x) = \cos(\pi x)$ to be retrieved, which is $O(1)$. With $\gamma = 0.05$, in Fig. 5 we show the residual errors, $s$ and $a_0$, while in Fig. 6(a) we plot the numerical errors, which are smaller than 0.06. In addition that very near the initial time, all the errors are very small.

In another test we employ the $\eta$ in Eq. (39) with $\gamma_1 = 0.97$ and $\gamma_2 = 10^{-6}$. In Fig. 7 we show the residual errors, $s$ and $a_0$, while in Fig. 6(b) we plot the numerical errors, which are smaller than 0.056. It is better than the above results. Also the residual errors are better than the above computations.

Then we add a relative random noise with intensity 10% in the final data, and in Fig. 8(a) we show the numerical errors, which are smaller than 0.06. It indicates that the present algorithm is robust against noise.

The main drawback of the above computation is that it converges quite slowly, which is due to the fact that the coefficient matrix $\mathbf{B}$ is full by using the MFS. By

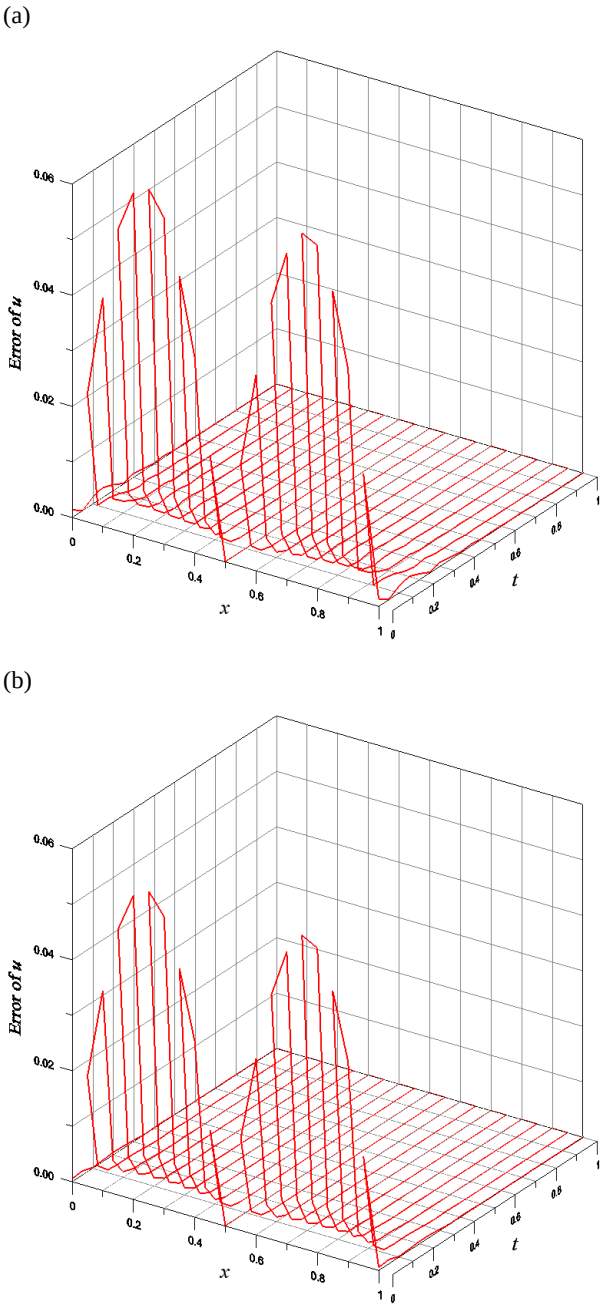


Figure 6: Showing numerical error for the backward heat conduction problem calculated by the RSDM: (a) a constant $\eta$, and (b) an exponential $\eta$.

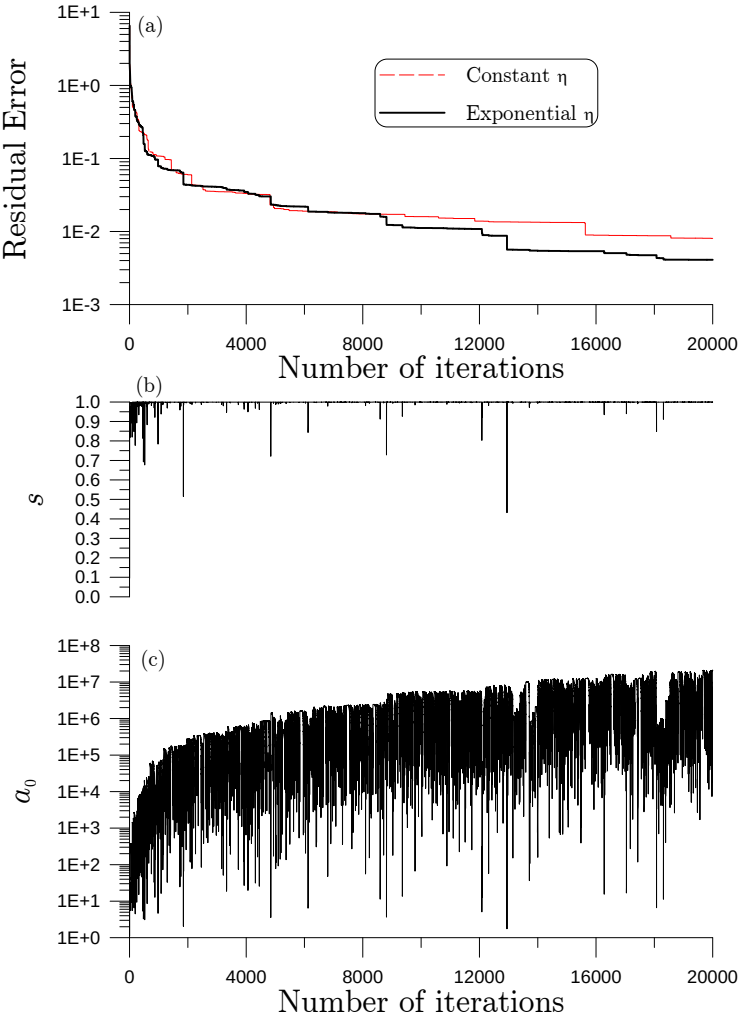


Figure 7: For example 4 showing (a) the residual errors, (b) $s$, and (c) $a_0$ for exponential $\eta$.

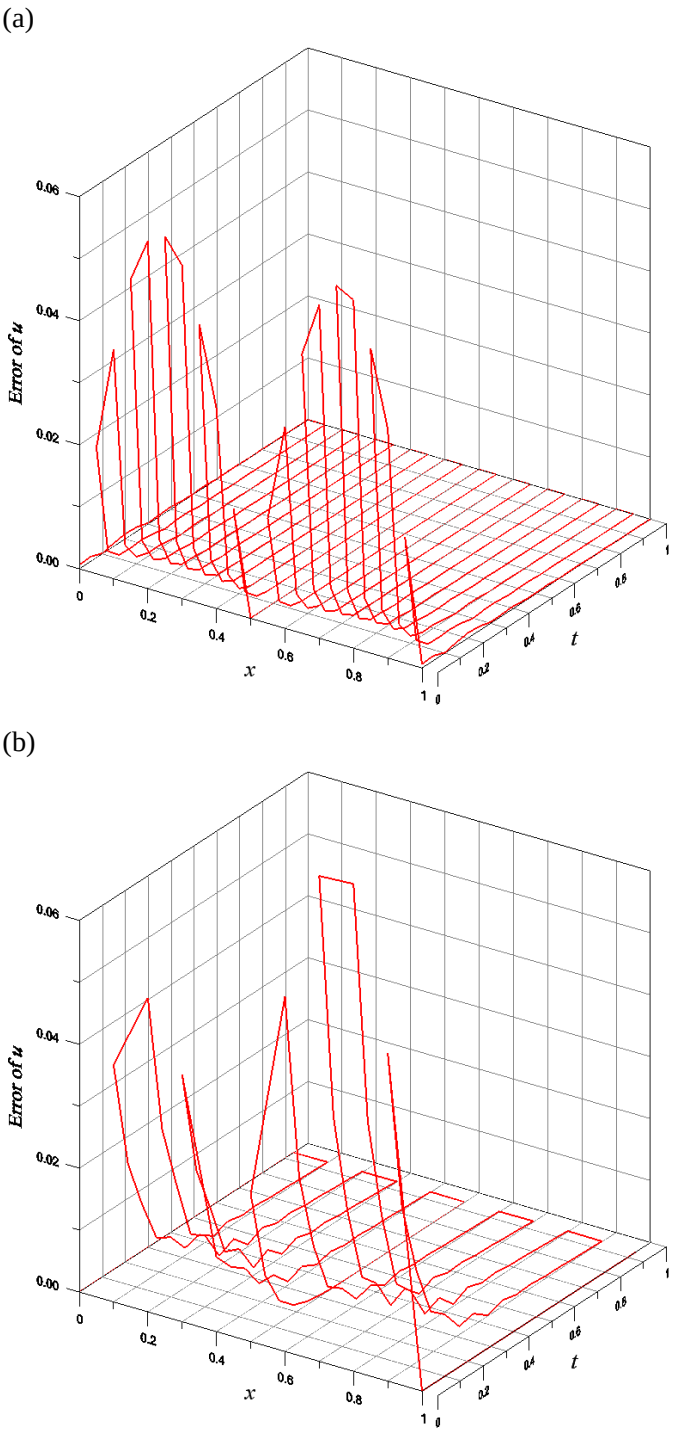


Figure 8: Showing the numerical errors for the backward heat conduction problem calculated by the RSDM: (a) MFS, and (b) Finite Difference.

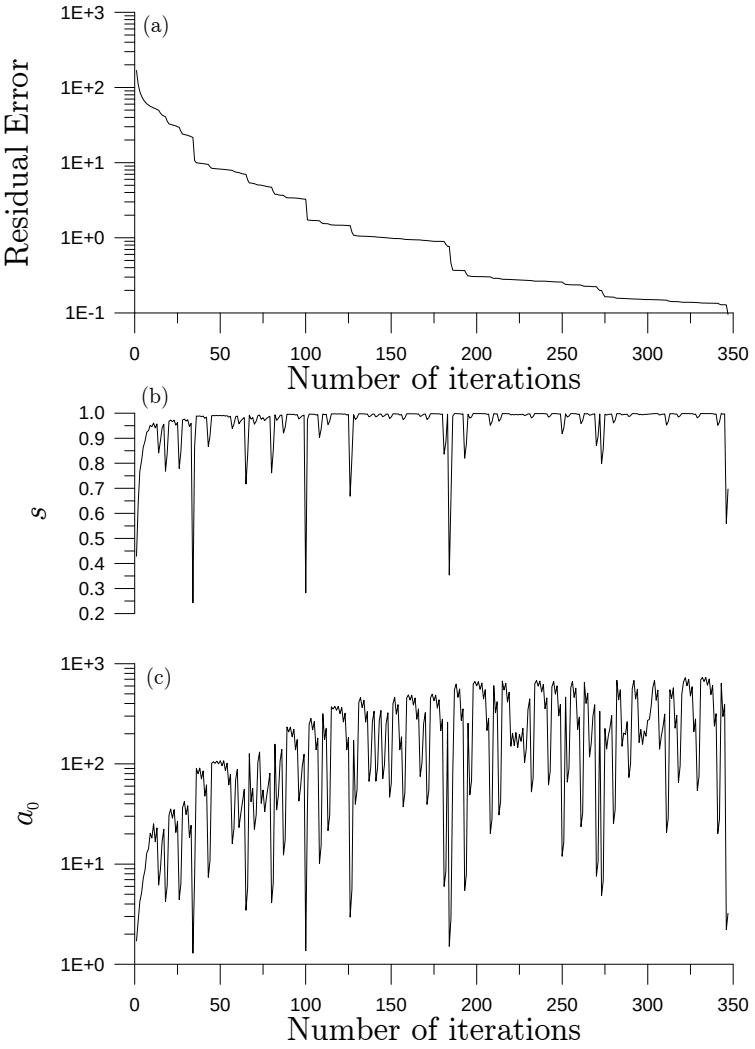


Figure 9: For example 4 with finite difference showing (a) the residual errors, (b) $s$, and (c) $a_0$.

applying the new algorithm RSDM to solve the same backward heat conduction problem we can use, instead of the MFS, the finite difference approximation of Eq. (48):

$$\alpha \frac{u_{i+1,j} - 2u_{i,j} + u_{i-1,j}}{(\Delta x)^2} - \frac{u_{i,j+1} - u_{i,j}}{\Delta t} = 0. \tag{56}$$

We fix $\Delta x = 1/n_1$ and $\Delta t = 1/n_2$, where $n_1 = 11$ and $n_2 = 16$ are numbers of nodal points. Under the same noise intensity added in the data, we apply the RSDM with $\gamma = 0.15$ to solve this problem, which is convergent faster only through 347 step as shown in Fig. 9 for displaying the residual error, $s$ and $a_0$. In Fig. 8(b) we show the numerical errors, which are smaller than 0.0752. It indicates that the present algorithm is robust against noise.

### 4.3 Example 5

In this example we consider a two-dimensional but highly ill-conditioned linear system:

$$\begin{bmatrix} 2 & 6 \\ 2 & 6.0001 \end{bmatrix} \begin{bmatrix} x \\ y \end{bmatrix} = \begin{bmatrix} 8 \\ 8.0001 \end{bmatrix}. \tag{57}$$

The condition number of this system is $\mathrm{Cond}(\mathbf{B}^{\mathrm{T}}\mathbf{B}) = 1.596 \times 10^{11}$, where $\mathbf{B}$ denotes the coefficient matrix . The exact solution is $(x,y) = (1,1)$.

Now we fix the noise to be 0.01, $\varepsilon = 10^{-8}$ and starting from an initial condition $(x_0, y_0) = (0.5, 0.5)$. By applying the Barzilai-Borwein method (BBM), it does not converge with 2000 iterations, and obtain an inaccurate solution of $(x,y) = (0.7, 1.1)$. The $a_0$ of BBM is shown in Fig. 10(b) by the dashed line. When $\gamma = 0$ the novel algorithm led to an incorrect solution of $(x,y) = (136.22, -44.1)$, whose $a_0$ is shown in Fig. 10(b) by the solid line. Then we apply the novel algorithm with $\gamma = 0.2$ to this problem. It led to an approximate solution of $(x,y) = (1.004, 0.999)$ with maximum error being $4.47 \times 10^{-3}$. The iterative orbit obtained from the novel algorithm is shown in Fig. 10(a), while $a_0$ is shown in Fig. 10(b) by the dashed-dotted line. When the BBM and the novel algorithm with $\gamma = 0$ are easily disturbed by noise for the above ill-posed system, the novel algorithm with $\gamma > 0$ can work very well against the disturbance of noise. Both $a_0$ of the BBM and the SDM tend to a constant, and thus they cannot approach to the true solution.

### 4.4 Example 6

In this example we consider a linear system:

$$\begin{bmatrix} 20 & 0 & 0 & 0 \\ 0 & 10 & 0 & 0 \\ 0 & 0 & 2 & 0 \\ 0 & 0 & 0 & 1 \end{bmatrix} \begin{bmatrix} x_1 \\ x_2 \\ x_3 \\ x_4 \end{bmatrix} = \begin{bmatrix} 1 \\ 1 \\ 1 \\ 1 \end{bmatrix}. \tag{58}$$

The condition number of this system is $\mathrm{Cond}(\mathbf{B}) = 20$.

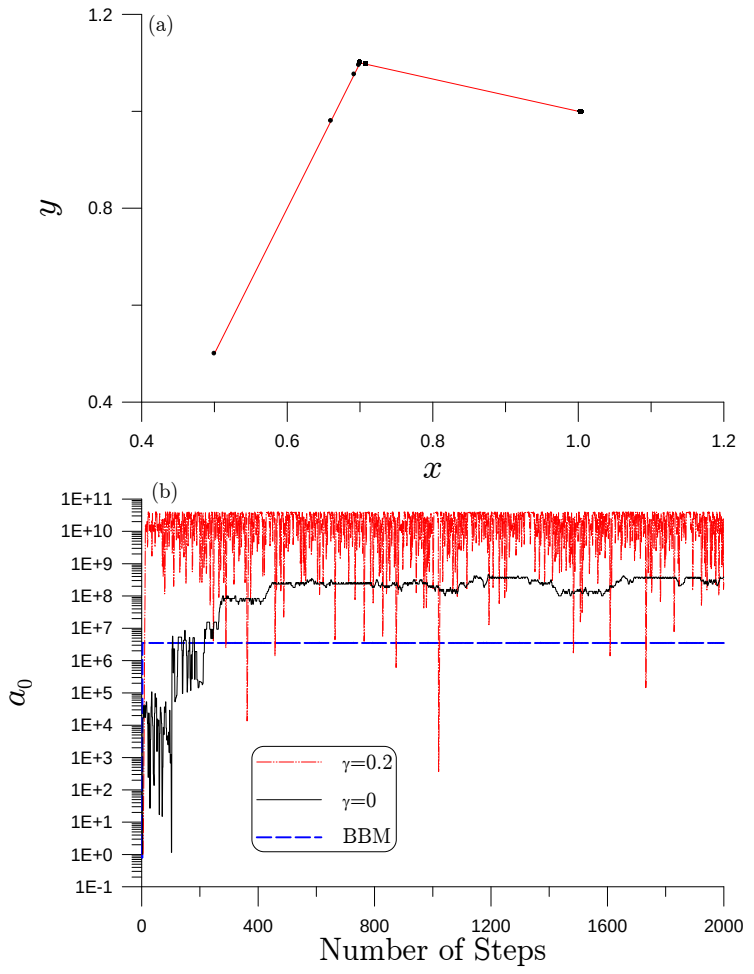


Figure 10: For example 5 (a) showing the iterative path obtained from the novel algorithm with $\gamma = 0.2$, and (b) comparing $a_0$ for different algorithms.

We found that the BBM is not applicable for many initial conditions of $x_i$. We choose $x_i = 1.2$. In Fig. 11 we compare the F-norm of $\|\mathbf{F}_k\|$ and residual errors $\|\mathbf{r}_k\|$ for the BBM and the RSDM in Section 3.4 under a stringent convergence criterion $\varepsilon = 10^{-15}$. For the RSDM we use $\gamma_1 = 0.95$ and $\gamma_2 = 10^{-2}$. It can be seen that the RSDM is very fast as the BBM is.

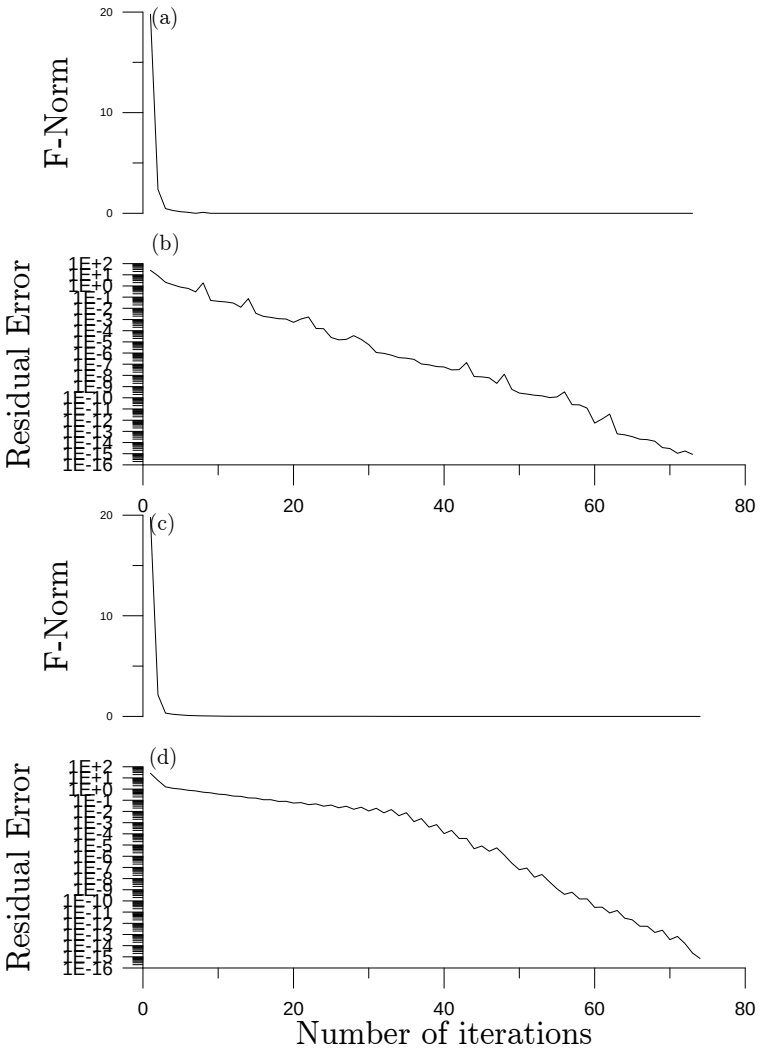


Figure 11: For example 6 showing the F-norms and the residual errors for (a) and (b) of the BBM, and (c) and (d) of the RSDM.

### *4.5 The first-kind Fredholm integral equation*

A possible application of the present RSDM is for solving the first-kind linear Fredholm integral equation:

$$\int_a^b K(s,t)x(t)dt = h(s),\ s \in [c,d], \tag{59}$$

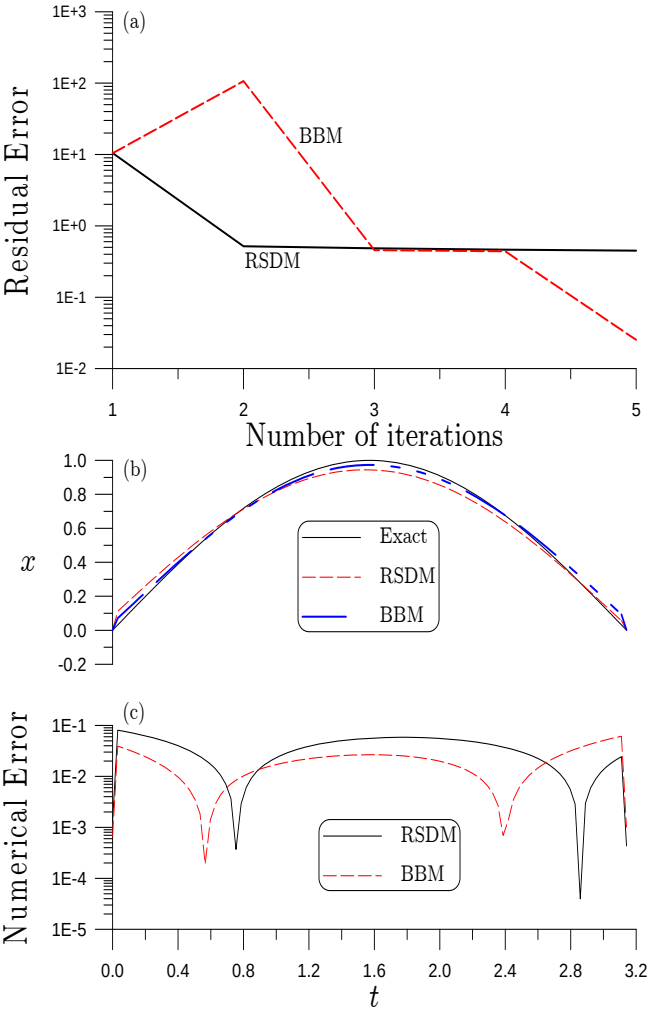


Figure 12: For the Fredholm integral equation: (a) showing the residual errors, (b) comparing numerical and exact solutions, and (c) displaying the numerical errors.

where $K(s,t)$ and $h(s)$ are known functions and $x(t)$ is an unknown function. We also suppose that $h(s)$ is perturbed by a random noise.

Let us discretize the intervals of $[a,b]$ and $[c,d]$ into $m_1$ and $m_2$ subintervals by noting $\Delta t = (b-a)/m_1$ and $\Delta s = (c-d)/m_2$. Let $x_j := x(t_j)$ be a numerical value of $x$ at a grid point $t_j$, and let $K_{i,j} = K(s_i,t_j)$ and $h_i = h(s_i)$, where $t_j = a+(j-1)\Delta t$

and $s_i = c + (i-1)\Delta s$. Through a trapezoidal rule, Eq. (59) can be discretized into

$$\frac{\Delta t}{2} K_{i,1} x_1 + \Delta t \sum_{j=2}^{m_1} K_{i,j} x_j + \frac{\Delta t}{2} K_{i,m_1+1} x_{m_1+1} = h_i,\ i = 1, \ldots, m_2 + 1, \tag{60}$$

which are linear algebraic equations denoted by

$$\mathbf{B}\mathbf{x} = \mathbf{b}_1, \tag{61}$$

where $\mathbf{B}$ is a rectangular matrix with dimensions $(m_2+1) \times (m_1+1)$. Here, $\mathbf{b}_1 = (h_1, \ldots, h_{m_2+1})^{\mathrm{T}}$, and

$$\mathbf{x} = (x_1, \ldots, x_{m_1+1})^{\mathrm{T}} \tag{62}$$

is the unknown vector. The data $h_j$ may be corrupted by noise:

$$\hat{h}_j = h_j + \sigma R(j). \tag{63}$$

We test our approach above, by considering the numerical solution of the following first-kind Fredholm integral equation:

$$\int_0^{\pi} e^{s \cos t} x(t) dt = \frac{2}{s} \sinh s,\ s \in [0, \pi/2], \tag{64}$$

which has an exact solution $x(t) = \sin t$. By fixing $m_1 = m_2 = 50$, and $\gamma = 0.35$ in the RSDM and under a noise with $\sigma = 0.01$ the numerical results are shown in Fig. 12 by (a) showing the residual error, (b) comparing numerical and exact solutions, and (c) displaying the numerical error, of which the numerical solution has a maximum error 0.07. For the purpose of comparison we also apply the BBM to this example, where the numerical results as shown in Fig. 12 are competitive to that of the RSDM.

## 5 Conclusions

In order to tackle the numerical instability of some conventional iterative methods to solve ill-posed linear problems, we have developed a new iterative algorithm, namely the relaxed steepest descent method (RSDM). This is the first time that one can derive the SDM with a relaxation factor from the viewpoint of ODEs and invariant manifold. In this new setting we can understand why the SDM converges very slowly, because there exists a *slow manifold* to drag the iterative orbit generated from the SDM. We have proved that the RSDM is unconditionally convergent. When the parameter $\gamma$ is given to be a positive value, the convergence speed is much

fast than that by using $\gamma = 0$ of the SDM. We also observed that when $\gamma$ varies from zero to a positive value, the iterative orbit undergoes a Hopf bifurcation and thus accompanied with an intermittent behavior. Through this bifurcation, the algorithm of RSDM can converge faster than the SDM. Several numerical examples were examined, some of which were compared with exact solutions, revealing that RSDM can work very well even for highly ill-conditioned linear equations under a large noise perturbation. We showed the advantage by using an exponential $\eta$ in Eq. (39) for the RSDM used in solving the BHCP. However, we need more study to propose a suitable strategy to suppress the value of $a_0$ to decrease the value of $s$.

**Acknowledgement:** Taiwan's National Science Council project NSC-100-2221-E-002-165-MY3 granted to the author is highly appreciated.

## References

**Absil, P.-A.; Baker, C. G.; Gallivan, K. A.** (2007): Trust-region methods on Riemannian manifolds. *Found. Comput. Math.*, vol. 7, pp. 303-330.

**Adler, R. L.; Dedieu, J.-P.; Margulies, J. Y.; Martens, M.; Shub, M.** (2002): Newton's method on Riemannian manifolds and a geometric model for the human spine. *IMA J. Numer. Anal.*, vol. 22, pp. 359-390.

**Baker, C. G.; Absil, P.-A.; Gallivan, K. A.** (2008): Implicit trust-region methods on Riemannian manifolds. *IMA J. Numer. Anal.*, vol. 28, pp. 665-689.

**Barzilai, J.; Borwein, J. M.** (1988): Two point step size gradient methods. *IMA J. Numer. Anal.*, vol. 8, pp. 141-148.

**Bhaya, A.; Kaszkurewicz, E.** (2006): Control Perspectives on Numerical Algorithms and Matrix Problems. SIAM, Advances in Design and Control 10.

**Brown, A. A.; Bartholomew-Biggs, M. C.** (1989): Some effective methods for unconstrained optimization based on the solution of systems of ordinary differential equations. *J. Optim. Theory Appl.*, vol. 62, pp. 211-224.

**Chang, C. W.; Liu, C.-S.** (2009): A fictitious time integration method for backward advection-dispersion equation. *CMES: Computer Modeling in Engineering & Sciences*, vol. 51, pp. 261-276.

**Chehab, J.-P.; Laminie, J.** (2005): Differential equations and solution of linear systems. *Numer. Algor.*, vol. 40, pp. 103-124.

**Chen, C. S.; Cho, H. A.; Golberg, M. A.** (2006): Some comments on the ill-conditioning of the method of fundamental solutions. *Eng. Anal. Bound. Elem.*, vol. 30, pp. 405-410.

**Chi, C. C.; Yeih, W.; Liu, C.-S.** (2009): A novel method for solving the Cauchy problem of Laplace equation using the fictitious time integration method. *CMES: Computer Modeling in Engineering & Sciences*, vol. 47, pp. 167-190.

**Eicke, B.; Louis, A. K.; Plato, R.** (1990): The instability of some gradient methods for ill-posed problems. *Numer. Math.*, vol. 58, pp. 129-134.

**Golberg, M. A.; Chen, C. S.** (1996): Discrete Projection Methods for Integral Equations. Computational Mechanics Publications, Southampton.

**Hanke, M.** (1991): Accelerated Landweber iterations for the solution of ill-posed problems. *Numer. Math.*, vol. 60, pp. 341–373.

**Hanke, M.** (1995): Conjugate gradient type methods for ill-posed problems. Longman, Harlow.

**Helmke, U.; Moore, J. B.** (1994): Optimization and Dynamical Systems. Springer, Berlin.

**Hoang, N. S.; Ramm, A. G.** (2008): Solving ill-conditioned linear algebraic systems by the dynamical systems method (DSM). *J. Inv. Prob. Sci. Eng.*, vol. 16, pp. 617-630.

**Hoang, N. S.; Ramm, A. G.** (2010): Dynamical systems gradient method for solving ill-conditioned linear algebraic systems. *Acta Appl. Math.*, vol. 111, pp. 189-204.

**Hon, Y. C.; Li, M.** (2009): A discrepancy principle for the source points location in using the MFS for solving the BHCP. *Int. J. Comput. Meth.*, vol. 6, pp. 181-197.

**Ku, C. Y.; Yeih, W.; Liu, C.-S.; Chi, C. C.** (2009): Applications of the fictitious time integration method using a new time-like function. *CMES: Computer Modeling in Engineering & Sciences*, vol. 43, pp. 173-190.

**Kunisch, K.; Zou, J.** (1998): Iterative choices of regularization parameters in linear inverse problems. *Inverse Problems*, vol. 14, pp. 1247-1264.

**Liu, C.-S.** (2000): Intermittent transition to quasiperiodicity demonstrated via a circular differential equation. *Int. J. Non-Linear Mech.*, vol. 35, pp. 931-946.

**Liu, C.-S.** (2001): Cone of non-linear dynamical system and group preserving schemes. *Int. J. Non-Linear Mech.*, vol. 36, pp. 1047-1068.

**Liu, C.-S.** (2005): Nonstandard group-preserving schemes for very stiff ordinary differential equations. *CMES: Computer Modeling in Engineering & Sciences*, vol. 9, pp. 255-272.

**Liu, C.-S.** (2007): A study of type I intermittency of a circular differential equation under a discontinuous right-hand side. *J. Math. Anal. Appl.*, vol. 331, pp. 547-566.

**Liu, C.-S.** (2008): A time-marching algorithm for solving non-linear obstacle prob-

lems with the aid of an NCP-function. *CMC: Computers, Materials & Continua*, vol. 8, pp. 53-65.

**Liu, C.-S.** (2009a): A fictitious time integration method for the Burgers equation. *CMC: Computers, Materials & Continua*, vol. 9, pp. 229-252.

**Liu, C.-S.** (2009b): A fictitious time integration method for solving delay ordinary differential equations. *CMC: Computers, Materials & Continua*, vol. 10, pp. 97-116.

**Liu, C.-S.** (2009c): A fictitious time integration method for a quasilinear elliptic boundary value problem, defined in an arbitrary plane domain. *CMC: Computers, Materials & Continua*, vol. 11, pp. 15-32.

**Liu, C.-S.** (2010): The fictitious time integration method to solve the space- and time-fractional Burgers equations. *CMC: Computers, Materials & Continua*, vol. 15, pp. 221-240.

**Liu, C.-S.** (2011): The method of fundamental solutions for solving the backward heat conduction problem with conditioning by a new post-conditioner. *Num. Heat Transfer, B: Fundamentals*, vol. 60, pp. 57-72.

**Liu, C.-S.; Atluri, S. N.** (2008): A novel time integration method for solving a large system of non-linear algebraic equations. *CMES: Computer Modeling in Engineering & Sciences*, vol. 31, pp. 71-83.

**Liu, C.-S.; Atluri, S. N.** (2009a): A Fictitious time integration method for the numerical solution of the Fredholm integral equation and for numerical differentiation of noisy data, and its relation to the filter theory. *CMES: Computer Modeling in Engineering & Sciences*, vol. 41, pp. 243-261.

**Liu, C.-S.; Atluri, S. N.** (2009b): A highly accurate technique for interpolations using very high-order polynomials, and its applications to some ill-posed linear problems. *CMES: Computer Modeling in Engineering & Sciences*, vol. 43, pp. 253-276.

**Liu, C.-S.; Atluri, S. N.** (2011): Simple "residual-norm" based algorithms, for the solution of a large system of non-linear algebraic equations, which converge faster than the Newton's method. *CMES: Computer Modeling in Engineering & Sciences*, vol. 71, pp. 279-304.

**Liu, C.-S.; Chang, C. W.** (2009): Novel methods for solving severely ill-posed linear equations system. *J. Marine Sci. Tech.*, vol. 9, pp. 216-227.

**Liu, C.-S.; Hong, H. K.; Atluri, S. N.** (2010): Novel algorithms based on the conjugate gradient method for inverting ill-conditioned matrices, and a new regularization method to solve ill-posed linear systems. *CMES: Computer Modeling in Engineering & Sciences*, vol. 60, pp. 279-308.

**Liu, C.-S.; Yeih, W.; Atluri, S. N.** (2009): On solving the ill-conditioned system $\mathbf{Ax} = \mathbf{b}$: general-purpose conditioners obtained from the boundary-collocation solution of the Laplace equation, using Trefftz expansions with multiple length scales. *CMES: Computer Modeling in Engineering & Sciences*, vol. 44, pp. 281-311.

**Luenberger, D. G.** (1972): The gradient projection method along geodesics. *Management Sci.*, vol. 18, pp. 620-631.

**Press, W. H.; Teukolsky, S. A.; Vetterling W. T.; Flannery, B. P.** (1992): Numerical Recipes in Fortran. The Art of Scientific Computing. Second Ed., Cambridge University.

**Resmerita, E.** (2005): Regularization of ill-posed problems in Banach spaces: convergence rates. *Inverse Problems*, vol. 21, pp. 1303-1314.

**Smith, S. T.** (1994): Optimization techniques on Riemannian manifolds: Hamiltonian and gradient flows, algorithms and control. *Fields Inst. Commun.*, vol. 3, pp. 113-136.

**Tikhonov, A. N.; Arsenin, V. Y.** (1977): Solutions of Ill-Posed Problems. John-Wiley & Sons, New York.

**Wang, Y.; Xiao, T.** (2001): Fast realization algorithms for determining regularization parameters in linear inverse problems. *Inverse Problems*, vol. 17, pp. 281-291.

**Xie, J.; Zou, J.** (2002): An improved model function method for choosing regularization parameters in linear inverse problems. *Inverse Problems*, vol. 18, pp. 631-643.

**Yang, Y.** (2007): Globally convergent optimization algorithms on Riemannian manifolds: Uniform framework for unconstrained and constrained optimization. *J. Optim. Theory Appl.*, vol. 132, pp. 245-265.